A study on attenuation correction using Tc-99m external TCT source in Tc-99m GSA liver SPECT

Yasuyuki Takahashi,* Kenya Murase,* Teruhito Mochizuki,** Hiroshi Higashino,***
Yoshifumi Sugawara** and Akiyoshi Kinda****

*Department of Medical Engineering, Division of Allied Health Sciences, Osaka University Graduate School of Medicine
**Department of Radiology, Ehime University School of Medicine
***Department of Radiology, Ehime Prefectural Imabari Hospital
****Toshiba Medical Engineering Laboratory

Purpose: In attenuation correction of ECT images by transmission CT (TCT) with an external ^{99m}Tc γ-ray source, simultaneous TCT/ECT data acquisition is difficult, when the same radionuclide such as ^{99m}Tc-tetrofosmin or ^{99m}Tc-GSA is used as the tracer. In this case, TCT is usually acquired before administration of the tracer, and ECT is acquired separately after the tracer injection. However, misregistration may occur between the TCT and ECT images, and the repetition of examinations add to the mental and physical stress of the patients. In this study, to eliminate this problem, we evaluated whether attenuation correction of ECT images can be achieved by acquiring TCT and ECT simultaneously, then acquiring ECT alone, and preparing an attenuation map by subtracting the latter from the former using ^{99m}Tc-GSA liver ECT. ***Method:*** The ECT system used was a three-head gamma camera equipped with one cardiac fan beam collimator and two parallel beam collimators. External γ-ray source for TCT of ^{99m}Tc was 740 MBq, and ECT of ^{99m}Tc-GSA was 185 MBq. First, pure TCT data were acquired for the original TCT-map, then, ECT/TCT data were acquired for the subtracted TCT-map, and finally, pure ECT data were acquired. The subtracted attenuation map was produced by subtracting the pure ECT image from the TCT/ECT image, and attenuation correction of the ECT image was done using both this subtracted TCT map and attenuation map from pure TCT. These two attenuation corrected images and non-corrected images were compared. Hot rods phantom, a liver phantom with a defect, and 10 patients were evaluated. ***Results:*** Attenuation corrected ECT values using the subtraction attenuation map showed an error of about 5% underestimation compared with ECT values of the images corrected by original attenuation map at the defect in the liver phantom. A good correlation of $y = 22.65 + 1.06x$, r = 0.958 was observed also in clinical evaluation. ***Conclusion:*** By means of the method proposed in this study, it is possible to perform simultaneous TCT/ECT data acquisition for attenuation correction using Tc-99m external source in Tc-99m GSA liver SPECT. Moreover, it is thought that this method decreases the mental and physical stress of the patients.

Key words: transmission computed tomography, ^{99m}Tc-GSA, subtraction attenuation map

INTRODUCTION

Recently, ^{99m}Tc preparations, which are convenient for emergency examinations, are commonly used as tracers for nuclear medicine examinations, e.g. ^{99m}Tc-HM-PAO for imaging of the cerebral blood flow and ^{99m}Tc-tetrofosmin for imaging of myocardial perfusion. For transmission computed tomography (TCT), ^{99m}Tc is also used as a relatively available external source.[1,2] However,

if the same nuclide is used, TCT and ECT must be acquired separately. But the effects of the registration errors between TCT and ECT images, and the repetition of examinations increases the mental and physical stress of the patients.

TCT/ECT simultaneous acquisition can be performed by SPECT/CT system, or TCT (Gd-153)/ECT (Tc-99m) dual-isotope SPECT; however, the radioactive half life of ^{153}Gd of external source in these systems is as short as 240 days, and these isotopes are expensive. Therefore, if Tc-99m is used as an external source, attenuation correction could be performed easily at a low cost, although there is a problem with the present regulation system. To avoid mis-registration, it is necessary to perform TCT and ECT in the simultaneous mode.[3]

In this study, we, therefore, evaluated the feasibility of the method in which TCT and ECT are acquired simultaneously, then ECT alone is performed, using the same Tc-99m as the radiopharmaceuticals for imaging and a TCT map, which was generated by subtracting the latter from the former. ECT is corrected using this map. In this study, the effect of attenuation correction by this method was evaluated by comparing images a TCT alone to obtain an original attenuation map before the injection of the tracer for simultaneous TCT and ECT and comparing the results of correction using this original attenuation non-corrected and corrected by the subtraction TCT map and by the original TCT map.

MATERIALS AND METHODS

ECT system and condition
The ECT system used was a GCA-9300A/UI (Toshiba Medical Systems, Tochigi, Japan) equipped with one cardiac fan beam collimator and two parallel beam collimators, with the data processor also Toshiba, GMS-5500A/PI. The TCT external γ-ray source was a sheet-shape made from a bellows tube filled with 740 MBq of ^{99m}Tc. The tube was 1 mm in the inner diameter made of fluorocarbon resin embedded in an acrylic rectangular board of 250×100 mm.

Both TCT and ECT images were sampled with a matrix size of 128×128, continuous mode (15 min/rotation) at intervals of 6 degrees (60 directions, 360-degree acquisition/detector). The pixel size was 3.2 mm. With these parameters, the count per detector in the phantom study was about 75 counts/pixel; and the counts/pixel in the myocardial area of patients was higher than 120. According to the triple-energy window (TEW) method,[4] the acquisition window widths were 20% for the main window at 140 keV of ^{99m}Tc and 7% for the lower subwindow.

After truncation correction, attenuation maps of TCT acquisition data[5] were produced by the filtered back projection (FBP) method. Subsequently, parallel beam projection data of the 2 detectors for ECT imaging were summated, then TEW scatter correction (SC) was performed and ECT images were reconstructed using Ordered Subsets-Expectation Maximization (OS-EM).[6–8]

The ECT acquisition data were reconstructed with a ramp convolution filter, and high frequency noise was decreased with post-reconstruction Butterworth filtering (cutoff frequency = 0.44 cycle/cm).

Data acquisition and imaging protocols
In the phantom study, ^{99m}Tc was filled in the phantom, then, protocol A′ (TCT + ECT) was acquired with the external source, followed by protocol A″ (ECT only) which was acquired without the external source. Then, a subtraction attenuation map (S-Map) was generated by subtracting data (protocol A′ – protocol A″), and attenuation corrected ECT images of the protocol A″ were reconstructed. In the phantom study, the phantom was left as it was for four days, a TCT source was placed again after 96 hours, then protocol A (TCT only) was acquired. An original attenuation map (O-Map) was generated by protocol A alone.
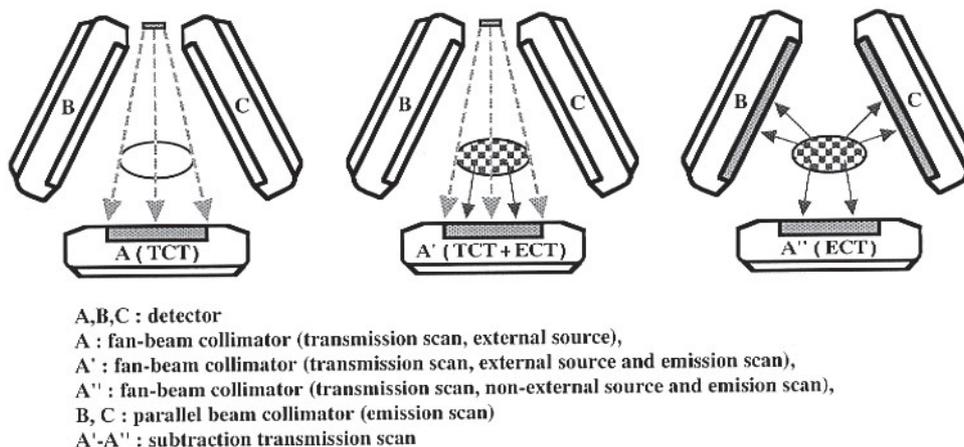

A,B,C : detector
A : fan-beam collimator (transmission scan, external source),
A′ : fan-beam collimator (transmission scan, external source and emission scan),
A″ : fan-beam collimator (transmission scan, non-external source and emision scan),
B, C : parallel beam collimator (emission scan)
A′-A″ : subtraction transmission scan

Fig. 1 The all directions method of data acquisition is shown.
(a) original TCT, (b) TCT and ECT simultaneous acquisition, (c) ECT
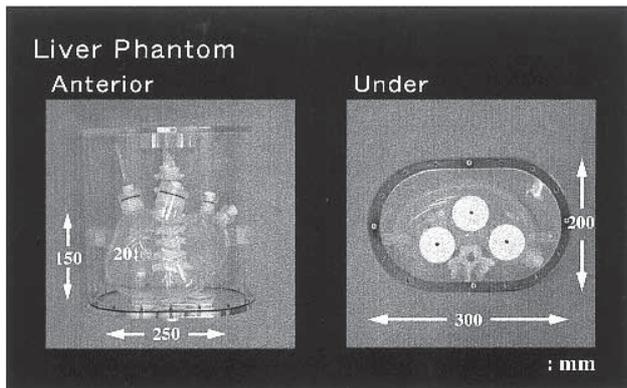
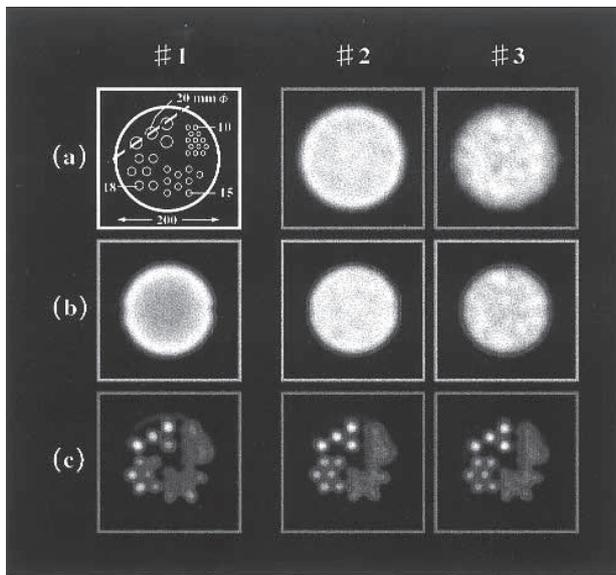Fig. 2 The appearance of the liver phantom.

Fig. 3 (a) A scheme and an attenuation map of the columnar phantom, (b) a SPECT image of a uniformity phantom, and (c) a SPECT image of a hot rods phantom. #1: No attenuation correction. #2: Original TCT. #3: Subtraction TCT.

In the human study, protocol A was acquired first, then protocol A′ was acquired, and finally protocol A″ was acquired. Attenuation corrected ECT images of the protocol A″ reconstructed using O-Map and S-Map were compared (Fig. 1). The acquisition time was 15 minutes in all cases.

Phantom study
In the cylindrical phantom (200 mm × 200 mm × 200 mm circle, AZ-660, Anzai-Sogyo, Tokyo, Japan), areas filled with uniform tracer activity (92.5 kBq/ml) and hot rods areas (9.25 kBq/ml) were created, and the image quality was compared using uniformity and hot rods (#1 (a) in Fig. 3). The ECT images after attenuation correction using the S-Map and O-Map were compared with the uniformity phantom with the profile curves and normal-
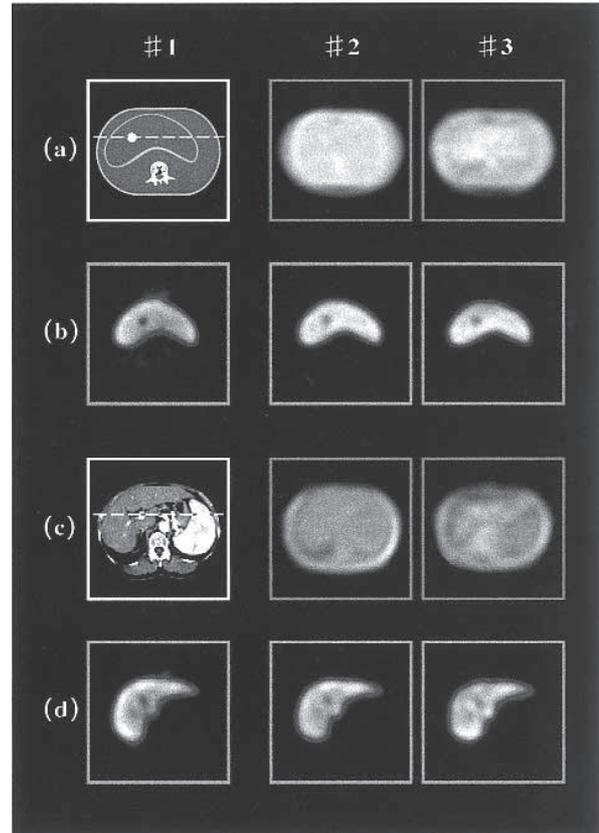

Fig. 4 (a) Schemes and attenuation maps of the liver phantom and a clinical case, (b) phantom SPECT images. (c) abdomen (liver) CT images and (d) abdomen (liver) ECT images. #1: No attenuation correction. #2: Original TCT. #3: Subtraction TCT.

ized root mean square errors (NRMSE (%), $\sqrt{[\Sigma(X_i - O_i)^2/\Sigma O_i^2]} \times 100$; X_i, subtraction image; O_i, original image; i, pixel number ($i = 1 - n$)). Spatial resolution of the hot rods phantom was evaluated with the profile curves.

In the liver phantom (LSF-type, Kyoto-Kagaku, Kyoto, Japan, Fig. 2), the concentration of ^{99m}Tc in the liver part was 247 kBq/ml[9] and the body part was 24.7 kBq/ml. In this study, a spherical defect of 20 × 20 mm in diameter was established in the left lobe, and ECT images after attenuation correction using S-Map and O-Map were compared with regard to the clarity of the defect image using profile curves.

Human study
As a human study, a 60-year-old female patient with liver cirrhosis diagnosed on the basis of clinical and CT findings was evaluated. The acquisition times of ECT and TCT were the same. Before administration of ^{99m}Tc-GSA, transmission data (protocol A) were acquired first. Then, 15 minutes after the intravenous injection of 185 MBq of ^{99m}Tc-GSA, simultaneous TCT/ECT data (protocol A′) were acquired with an external source (740 MBq of ^{99m}Tc). Finally, only ECT data (protocol A″) of ^{99m}Tc-GSA were acquired without an external source (Fig. 1).
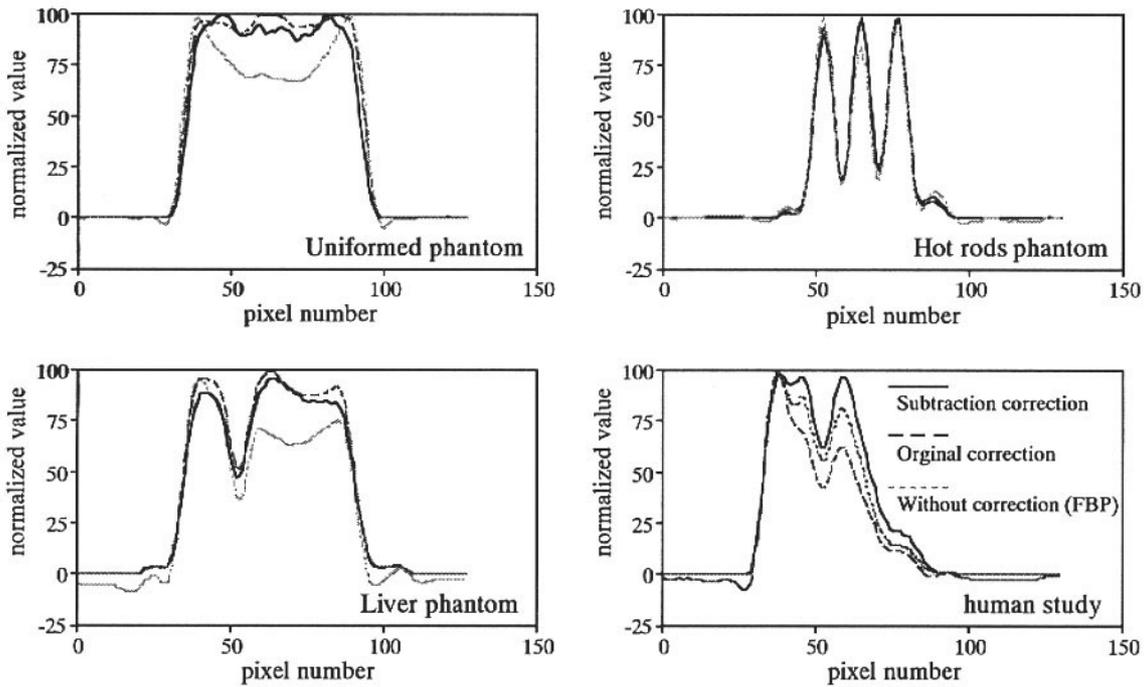
Fig. 5 CPR at the dotted line in each scheme. *Upper left*, uniformity phantom; *upper right*, hot rods phantom; *lower left*, liver phantom; *lower right*, case study.

S-Map was prepared by the subtraction, and O-Map was prepared from protocol A. In protocol A and protocol A″, 4 markers were placed on the body surface as the landmarks for the Automatic Registration Tool (ART),[10] and ECT images after attenuation correction using S-Map and O-Map were compared.

Human materials consisted of 10 patients (7 liver cirrhosis [4 males and 3 females aged 65 ± 6 years], and 3 hepatocellular carcinoma [2 males and 1 females aged 67 ± 5 years]).

RESULTS

Phantom study
The transaxial images of the uniformity phantom are shown in Figure 3 (b), and the place for the count profile curves (Table 1, *upper left*) shown as the broken line #1 (a) in Figure 3. The ECT values (mean ± SD, [CV(%)]) are for the internal side at both ends of the transaxial image: O-map 92.33 ± 3.52 [3.81], S-map 95.96 ± 1.94 [2.02], and ECT values without attenuation correction were 78.54 ± 15.60 [19.86]. ECT values using the S-Map was overestimated by about 9% near the center. The NRMSE in these images were 10.5%.

Figure 3 (c) shows the transaxial images of the hot rods phantom. The profile curves (Fig. 5, *upper right*) were nearly identical. Visualization was similar.

Defect in the liver phantom was shown as dotted lines in the scheme. Normalized ECT values of the defects (minimum value) using the S-Map were 10% better than
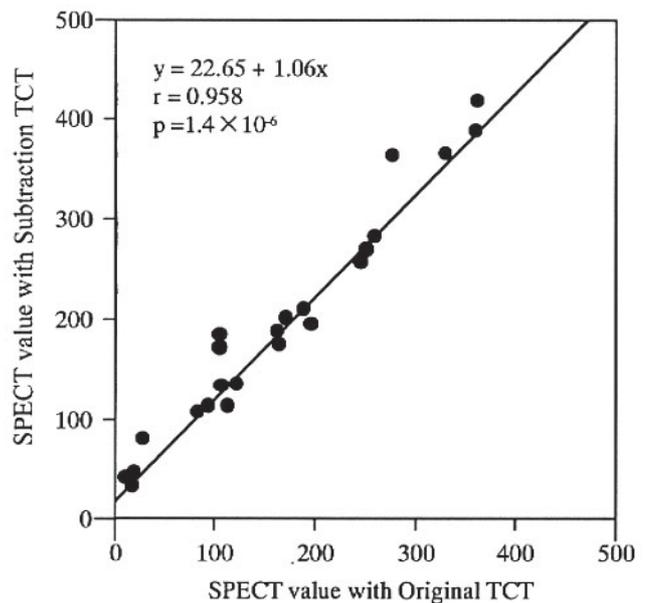

Fig. 6 Comparison of ECT values in 25 ROI including SOL and hepatectomy sites in 10 patients.

those using the O-Map (Fig. 5, *lower left*). Over correction of 4–7% was observed in the center and peripheries (Fig. 5, *upper right*).

Human study
The case (Fig. 4) presented here had liver cirrhosis with mild swelling of the left lobe. After angiography, a defect

of GSA was noted at the porta hepatis. The normalized ECT value of the defect (CPR in the area surrounded by the dotted line in the scheme; Fig. 5, *lower right*) was reduced by 10% with the S-Map as compared with the O-Map. In the caudate lobe, a 12% overestimation was observed.

In the 25 ROIs in 10 patients, the ECT values after attenuation correction using the O-Map and S-Map showed a good correlation ($y = 22.65 + 1.06x$, r = 0.958, p = 1.4 × 10^{-6}).

DISCUSSION

For attenuation correction of ECT images by TCT with an external source, TCT with ^{153}Gd can be acquired in combination with ECT simultaneously using tracers such as ^{201}Tl and ^{99m}Tc-MIBI in myocardial scintigraphy.[11] In an evaluation using TCT in the liver,[12] good quantitative results of volume measurements were reported.[13] In a liver ^{99m}Tc-GSA scintigraphy which is an analog ligand of the asialoglycoprotein receptor, it is report and attenuation correction is necessary in the quantitative evaluation of the liver.[14]

^{99m}Tc can also be used as an external source for TCT; however, TCT/ECT simultaneous acquisition[2] can not be used, when the same ^{99m}Tc radiotracer such as ^{99m}Tc-GSA is used. In the sequential mode,[14] TCT must be acquired before the administration of the tracer, and ECT thereafter can be acquired. However a mis-registration may between when TCT and ECT images for attenuation correction.[15] The mis-registration must be avoided by use of the ART method.[11] In sequential mode, improvement of concentration linearity was reported by combination of TCT attenuation correction and TEW scatter compensation.[14] Since the external source is comparatively large, TEW scatter compensation can also correct ECT scatter as well as TCT scatter.[16]

In order to reduce the repetition of examinations, we examined whether attenuation correction can be performed by acquiring TCT and ECT twice serially in the simultaneous mode and acquiring an attenuation map by image subtraction. When the protocol "simultaneous TCT/ECT (^{99m}Tc-GSA) followed ECT", i.e., (1) i.v. of radiotracer, (2) waiting for fixation of the radiotracer, (3) TCT/ECT, (4) ECT, subtracted TCT map (TCT/ECT − ECT) can be generated. This protocol saves the time needed for fixation of the radiotracer, compared with the conventional protocol "TCT (GSA) followed ECT", i.e., (1) TCT, (2) i.v. of radiotracer, (3) waiting for fixation, (4) ECT. In the phantom study, to minimize mis-registration between the ECT and TCT images, TCT and ECT were acquired simultaneously, ECT alone was then acquired, and original TCT was acquired after the phantom was allowed to stand for 96 hours in consideration of the attenuation time. However, as this protocol is difficult in clinical cases, markers were placed at 4 points on the

phantom, and images were overlayed by the landmark method of the ART.[10] In the experiments using uniformity, hot rods and liver phantoms, no marked difference was observed between the O-map and S-map, and a 5% error was observed in the defect value in the liver phantom with a model SOL. In human study, also, errors of ECT values in the defects after hepatectomy and relatively large SOL (space occupying lesion) of 3 cm or greater in diameter were 0–7%, but they were larger and more variable with a maximum of 20% for small tumors about 1 cm in diameter or other hepatic resions. Since this value was within the limits of agreement (mean ± 2SD) of the evaluation method of Bland & Altman,[17] it is clinically acceptable. However, there was no such error in the phantom study, and therefore, a part of the errors may due to respiration, which is uncorrectable by the subtraction method. Evaluation of the respiratory affect and its correction must be performed using respiratory gated[18] liver SPECT in future studies.

The subtraction method in ^{99m}Tc-GSA must take pharmacokinetic analyses into consideration; namely the liver is described in 30 seconds after injection, the tracer is accumulated rapidly, and after 15 to 40 minutes has comparatively little change in time-activity.[19] Therefore, TCT and ECT were acquired at the same time. Moreover, time-activity is considered to decrease more by acquiring continuous repetitive rotation of the gamma camera.[20] Since about 50% of the amount of administered ^{99m}Tc-GSA is accumulated in the liver,[19] sufficient radiotracer counts are obtained in the liver ECT may be obtained using one detector with parallel beam collimator. Then two other detectors may be used for TCT with high radioactivity counts. This method may improve the accuracy of TCT attenuation correction.

CONCLUSION

By means of the subtraction attenuation correction method proposed in this study, it is possible to perform simultaneous TCT/ECT data acquisition for attenuation correction using Tc-99m external source in Tc-99m GSA liver SPECT. Moreover, it is thought that this method decreases the mental and physical surden of the patients.

REFERENCES

1. Murase K, Tanada S, Inoue T, Sugawara Y, Hamamoto K. Improvement of brain single photon emission tomography (SPET) using transmission data acquisition in a four-head SPET scanner. *Eur J Nucl Med* 1993; 20: 32–38.
2. Jaszczak RJ, Gilland DR, Hanson MW, Jang S, Greer KL, Coleman RE. Fast Transmission CT for Determining Attenuation Maps Using a Collimated Line Source, Rotatable Air-Copper-Lead Attenuators and Fan-Beam Collimation. *J Nucl Med* 1993; 34: 1577–1586.
3. Ficaro EP, Fessler JA, Ackermann RJ, Rogers WL, Corbett JR, Chwaiger M. Simultaneous transmission-emission

thallium-201 cardiac SPECT: effects of attenuation correction on myocardial tracer distribution. *J Nucl Med* 1995; 36: 921–931.

4. Ogawa K. Simulation study of triple-energy-window scatter correction in combined Tl-201, Tc-99m SPECT. *Ann Nucl Med* 1995; 8: 277–281.

5. Motomura N, Ichihara T, Takayama T, Nishihara K, Inouye T, Kataoka T, et al. Practical method for reducing truncation artifacts in a fan beam transmission CT system. *J Nucl Med* 1998; 39: (Suppl) 178.

6. Hudson HM, Larkin RS. Accelerated image reconstruction using ordered subsets of projection data. *IEEE Trans Med Imaging* 1994; MI-13: 601–609.

7. Murase K, Tanada S, Sugawara Y, Tauxe WN, Hamamoto K. An evaluation of the accelerated expectation maximization algorithms for single-photon emission tomography image reconstruction. *Eur J Nucl Med* 1994; 21: 597–603.

8. Takahashi Y, Murase K, Higashino H, Sogabe I, Sakamoto K. Receiver operating characteristic (ROC) analysis of image reconstructed with iterative expectation maximization algorithms. *Ann Nucl Med* 2001; 15: 521–525.

9. Torizuka K, Ha-Kawa SK, Ikekubo K, Suga Y, Tanaka Y, Hino M, et al. Phase I clinical study on ^{99m}Tc-GSA, a new agent for functional imaging of the liver. *KAKU IGAKU (Jpn J Nucl Med)* 1991; 28: 1321–1331. (in Japanese)

10. Ardekani BA, Braun M, Hutton BF, Kanno I, Iida H. A Fully Automatic Multimodality Image Registration Algorithm. *J Comput Assist Tomogr* 1995; 19: 615–623.

11. Laere DL, Koole M, Kauppinen T, Monsieurs M, Bouwens L, Dierck R. Nonuniform Transmission in Brain SPECT Using ^{201}Tl, [153]Gd, and [99m]Tc Static Line Sources: Anthropomorphic Dosimetry Studies and Influence on Brain Quantification. *J Nucl Med* 2000; 41: 2051–2062.

12. Malko JA, Van Heertum RL, Gullberg GT, Kowalsky WP. SPECT liver imaging using an iterative attenuation correction algorithm and external flood source. *J Nucl Med* 1986; 27: 701–705.

13. Strauss LG, Clorius JH, Frank T, Van Kaick G. Single photon emission computerized tomography (SPECT) for estimates of liver and spleen volume. *J Nucl Med* 1984; 25: 81–85.

14. Ichihara T, Maeda H, Yamakado K, Motomura N, Matsumura K, Takeda K, et al. Quantitative analysis of scatter- and attenuation-compensated dynamic single-photon emission tomography for functional hepatic imaging with a receptor-binding radiopharmaceutical. *Eur J Nucl Med* 1997; 24: 59–67.

15. Murase K, Tanada S, Inoue T, Sugawara Y, Hamamoto K. Effect of misalignment between transmission and emission scans on SPECT images. *J Nucl Med Technol* 1993; 21: 152–156.

16. Matsumoto M, Kojima A, Ooyama Y, Kira T, Kira M, Yokoyama T, et al. An investigation of the scatter from TCT data using sheet source and its compensation. *KAKU IGAKU (Jpn J Nucl Med)* 1997; 34: 701. (in Japanese)

17. Bland JM, Altman DG. Statistical methods for assessing agreement between two methods of clinical measurement. *Lancet* 1986; 1: 307–310.

18. Cho K, Kumita S, Okada S, Kumazaki T. Development of respiratory gated myocardial SPECT system. *J Nucl Cardiol* 1999; 6: 20–28.

19. Ha-kawa SK, Nakanishi K, Kojima M, Tanaka Y, Kitagawa S, Kubota Y, et al. Clinical application of asialoglycoprotein receptor-mediated liver scintigraphy using ^{99m}Tc-DTPA-galactosyl-human serum albumin. *Jpn J Radiol Soc* 1991; 51: 1489–1497. (in Japanese)

20. Takahashi Y, Matsuki H, Mochizuki T. Basic study of continuous repetitive data acquisition using a phantom. *KAKU IGAKU (Jpn J Nucl Med)* 1996; 33: 1363–1369. (in Japanese)